

# Phase-sensitive order parameter symmetry test experiments utilizing $\text{Nd}_{2-x}\text{Ce}_x\text{CuO}_{4-y}/\text{Nb}$ zigzag junctions

Ariando, D. Darminto,\* H. -J. H. Smilde,† V. Leca,‡ D. H. A. Blank, H. Rogalla, and H. Hilgenkamp  
Faculty of Science and Technology and MESA<sup>+</sup> Research Institute,  
University of Twente, P.O. Box 217, 7500 AE Enschede, The Netherlands  
(Dated: November 19, 2018)

Phase-sensitive order parameter symmetry test experiments are presented on the electron-doped high- $T_c$  cuprate  $\text{Nd}_{2-x}\text{Ce}_x\text{CuO}_{4-y}$ . These experiments have been conducted using zigzag-shaped thin film Josephson structures, in which the  $\text{Nd}_{2-x}\text{Ce}_x\text{CuO}_{4-y}$  is connected to the low- $T_c$  superconductor Nb via a Au barrier layer. For the optimally doped as well as for the overdoped  $\text{Nd}_{2-x}\text{Ce}_x\text{CuO}_{4-y}$  a clear predominant  $d_{x^2-y^2}$ -wave behavior is observed at  $T = 4.2$  K. Both compounds were also investigated at  $T = 1.6$  K, presenting no indications for a change to a predominant  $s$ -wave symmetry with decreasing temperature.

PACS numbers: 74.20.Rp, 74.72.Jt, 74.50.+r

The determination of the order parameter symmetry in the high temperature superconductors is an important step towards the identification of the mechanism of superconductivity in these materials. This includes its dependencies on the sign and density of the mobile charge carriers, on temperature and possible other parameters. For the hole-doped high temperature superconductors, such as  $\text{YBa}_2\text{Cu}_3\text{O}_7$ , a long-lasting debate on the order parameter symmetry was settled by the clear  $d_{x^2-y^2}$ -wave behavior displayed in various phase-sensitive symmetry test experiments, as reviewed in [1, 2]. For the electron-doped materials,  $\text{Ln}_{2-x}\text{Ce}_x\text{CuO}_{4-y}$ , with  $\text{Ln} = \text{La}, \text{Nd}, \text{Pr}, \text{Eu}$  or  $\text{Sm}$ ,  $y \approx 0.04$ , only a few phase-sensitive test experiments have until now been reported, all based on grain boundary Josephson junctions. Tsuei and Kirtley [3] described the spontaneous generation of half-integer flux quanta in  $\text{Nd}_{1.85}\text{Ce}_{0.15}\text{CuO}_{4-y}$  and  $\text{Pr}_{1.85}\text{Ce}_{0.15}\text{CuO}_{4-y}$  tricrystalline films at temperature  $T = 4.2$  K, presenting evidence for a  $d_{x^2-y^2}$ -wave order parameter symmetry. A similar conclusion was drawn by Chesca *et al.* [4] from the magnetic field dependence of the critical current for grain boundary-based  $\pi$ -SQUIDS in near optimally doped  $\text{La}_{2-x}\text{Ce}_x\text{CuO}_{4-y}$ , also at  $T = 4.2$  K.

In contrast to these phase-sensitive experiments, a substantial volume of more indirect symmetry test experiments exists for the electron-doped materials. The conclusions from these studies are varying. Behavior in line with an  $s$ -wave, or more general a nodeless, symmetry was reported *e.g.*, from the absence of a zero-bias conductance peak in  $\text{Nd}_{1.85}\text{Ce}_{0.15}\text{CuO}_{4-y}$  tunneling spectra at  $T \geq 4.0$  K [5, 6, 7] and from the temperature dependencies of the London penetration depth in  $\text{Pr}_{1.855}\text{Ce}_{0.145}\text{CuO}_{4-y}$  for  $1.6 \text{ K} < T < 24 \text{ K}$  [8], in  $\text{Pr}_{2-x}\text{Ce}_x\text{CuO}_{4-y}$  with varying Ce-content ( $0.115 \leq x \leq 0.152$ ) for  $0.5 \text{ K} < T$  [9], and in  $\text{Nd}_{1.85}\text{Ce}_{0.15}\text{CuO}_{4-y}$  for  $1.5 \text{ K} < T < 4 \text{ K}$  [10], in addition to several earlier studies [11, 12, 13]. On the other hand,  $d$ -wave like characteristics were reported *e.g.*, from the observed

gap-anisotropy in angle resolved photoemission spectroscopy on  $\text{Nd}_{1.85}\text{Ce}_{0.15}\text{CuO}_{4-y}$  at  $T = 10$  K [14, 15], the temperature dependence of the London penetration depth in optimally doped  $\text{Pr}_{2-x}\text{Ce}_x\text{CuO}_{4-y}$  and  $\text{Nd}_{2-x}\text{Ce}_x\text{CuO}_{4-y}$  ( $0.4 \text{ K} < T$ ) [16, 17] and from the observation of zero-bias conductance peaks in optimally doped  $\text{Nd}_{1.85}\text{Ce}_{0.15}\text{CuO}_{4-y}$  ( $T = 4.2$  K) [18] and  $\text{La}_{1.855}\text{Ce}_{0.105}\text{CuO}_{4-y}$  for  $4.2 \text{ K} < T < 29 \text{ K}$  [19].

Recently, a transition from  $d$ -wave behavior for underdoped materials to  $s$ -wave like behavior for the optimally doped and overdoped compounds was reported from the temperature dependence of the London penetration depth in  $\text{Pr}_{2-x}\text{Ce}_x\text{CuO}_{4-y}$  and  $\text{La}_{2-x}\text{Ce}_x\text{CuO}_{4-y}$  [8] and from point contact spectroscopy [20, 21]. Further, Balcı *et al.* [22] suggested a temperature-dependent change in the order parameter symmetry for optimally and overdoped  $\text{Pr}_{2-x}\text{Ce}_x\text{CuO}_{4-y}$ , with  $s$ -wave behavior at  $T = 2$  K and  $d$ -wave behavior at  $T \geq 3$  K, based on specific heat measurements.

In view of this still ongoing discussion, there is a need for further phase-sensitive experiments, and specifically to study possible changes with temperature and doping. Tsuei and Kirtley [3] and Chesca *et al.* [4] succeeded in performing the first phase-sensitive measurements on the electron-doped compounds based on grain boundary junctions. Geometrical restrictions and the intrinsically low critical current densities  $J_c$  of the grain boundaries make such experiments very challenging, especially for investigations on non-optimally doped compounds. It is therefore advantageous to also explore other Josephson junction configurations, with potentially higher  $J_c$ 's. In addition, it would be very fruitful to have a configuration for the symmetry test-experiment in which a large Josephson penetration depth, associated with a low  $J_c$ , presents an advantage rather than a difficulty. Both aspects are fulfilled in the experiment described in the following, based on zigzag-shaped Josephson contacts between  $\text{Nd}_{2-x}\text{Ce}_x\text{CuO}_{4-y}$  and Nb, separated by a Au barrier layer.

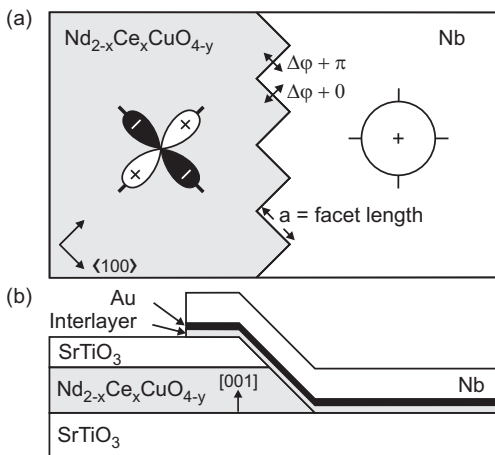


FIG. 1: (a) Schematic topview of a  $\text{Nd}_{2-x}\text{Ce}_x\text{CuO}_{4-y}/\text{Nb}$  zigzag structure with facet-length  $a$ . (b) Schematic sideview illustrating the ramp-type  $\text{Nd}_{2-x}\text{Ce}_x\text{CuO}_{4-y}/\text{Nb}$  Josephson junction.

The zigzag-configuration (Fig. 1(a)) has been described in detail in [23], where it was used to investigate symmetry admixtures in  $\text{YBa}_2\text{Cu}_3\text{O}_7$ . In these structures, all interfaces are aligned along one of the  $\langle 100 \rangle$ -directions of the cuprate, and are designed to have identical  $J_c$ -values. With the high- $T_c$  cuprate being an  $s$ -wave superconductor, the zigzag-structure presents no significant difference to the case of a straight junction aligned along one of the facet's directions. With the high- $T_c$  superconductor having a  $d_{x^2-y^2}$ -wave symmetry, the facets oriented in one direction experience an additional  $\pi$ -phase difference compared to those oriented in the other direction. For a given number of facets, the characteristics of these zigzag structures then depend on the ratio of the facet length  $a$  and the Josephson penetration depth  $\lambda_J$ , see *e.g.* [24]. In the small facet limit,  $a \ll \lambda_J$ , the zigzag structure can be envisaged as a one-dimensional array of Josephson contacts with an alternating sign of  $J_c$ , leading to anomalous magnetic field dependencies of the critical current, as displayed for  $\text{YBa}_2\text{Cu}_3\text{O}_7$  in Ref. [23]. In the large facet limit, the energetic groundstate includes the spontaneous formation of half-integer magnetic flux quanta at the corners of the zigzag structures, as seen in [25]. All experiments on  $\text{Nd}_{2-x}\text{Ce}_x\text{CuO}_{4-y}$  described below are in the small facet limit.

Figure 1(b) schematically shows the  $\text{Nd}_{2-x}\text{Ce}_x\text{CuO}_{4-y}/\text{Nb}$  ramp-type junctions that were used for the experiments. They were prepared by first depositing a bilayer of 150 nm  $[001]$ -oriented  $\text{Nd}_{2-x}\text{Ce}_x\text{CuO}_{4-y}$  and 35 nm  $\text{SrTiO}_3$  by pulsed laser deposition on a  $[001]$ -oriented  $\text{SrTiO}_3$  single-crystal substrate. For the optimally doped films a  $\text{Nd}_{1.85}\text{Ce}_{0.15}\text{CuO}_4$  target is used, for the overdoped case a  $\text{Nd}_{1.835}\text{Ce}_{0.165}\text{CuO}_4$  target. The  $\text{Nd}_{2-x}\text{Ce}_x\text{CuO}_{4-y}$

film is grown at 820 °C in 0.25 mbar of oxygen. Subsequently, the temperature is reduced to 740 °C for the growth of the  $\text{SrTiO}_3$  layer in 0.10 mbar of oxygen. Then the deposition chamber is evacuated to about  $10^{-6}$  mbar and the sample is kept at 740 °C for 10 – 15 minutes, before it is slowly cooled down to room-temperature under vacuum conditions. For the  $\text{Nd}_{1.85}\text{Ce}_{0.15}\text{CuO}_{4-y}$  films, this procedure yields a typical critical temperature  $T_c$  of 20 K, the  $\text{Nd}_{1.835}\text{Ce}_{0.165}\text{CuO}_{4-y}$  films had  $T_c$ 's of 13 K. The  $T_c$ 's for  $\text{Nd}_{1.85}\text{Ce}_{0.15}\text{CuO}_{4-y}$  and  $\text{Nd}_{1.835}\text{Ce}_{0.165}\text{CuO}_{4-y}$  were optimized with respect to the oxygen content. The next step in the junction fabrication process is the etching of a shallow ramp (15 – 20°) and cleaning of the sample using argon-ion milling, analogous to the procedure used for  $\text{YBa}_2\text{Cu}_3\text{O}_7$  [23, 26]. Then, using the same deposition and cool-down conditions as for the first  $\text{Nd}_{2-x}\text{Ce}_x\text{CuO}_{4-y}$  layer, a 12-nm  $\text{Nd}_{2-x}\text{Ce}_x\text{CuO}_{4-y}$  interlayer is deposited, followed by the in-situ pulsed-laser deposition of a 12-nm Au barrier layer at 100 °C. The interlayer, with the same composition as the base-layer, is employed to provide an in-situ formed interface between the cuprate layer and the Au-barrier. This is found to be of great importance in reaching high junction quality, as it was for the  $\text{YBa}_2\text{Cu}_3\text{O}_7$  case [23, 26]. Subsequently, a 160-nm Nb layer forming the counter electrode is deposited by dc-sputtering and structured by lift-off. Finally, the redundant, uncovered Au is removed by ion milling. In addition to zigzag structures with different size and number of facets, every chip contained several straight reference junctions oriented parallel to one of the facet directions.

The junctions were characterized by measuring the current-voltage ( $IV$ ) characteristics and the dependencies of the critical currents  $I_c$  on applied magnetic field  $H_a$ , using a four-probe method with the magnetic field parallel to the  $[001]$ -direction of the  $\text{Nd}_{2-x}\text{Ce}_x\text{CuO}_{4-y}$  in a well-shielded cryostat at  $T = 4.2$  K and  $T = 1.6$  K. For the determination of  $I_c$ , a typical voltage criterion of  $V_c \lesssim 2 \mu\text{V}$  was used. This yields a lower limit of  $V_c/R_n$  to  $I_c$ , with  $R_n$  being the junctions' normal state resistance. In the  $I_c(H_a)$ -dependencies presented here, the lowest  $I_c$  values can be considered as the lower limit in the determination of the critical current for that respective measurement.

Figure 2 shows the  $I_c(H_a)$ -dependence recorded for a 50  $\mu\text{m}$  wide straight  $\text{Nd}_{1.85}\text{Ce}_{0.15}\text{CuO}_{4-y}/\text{Nb}$  reference junction at  $T = 4.2$  K, and in the inset its zero-field  $IV$ -characteristic. The  $I_c(H_a)$ -dependence closely resembles a Fraunhofer pattern, which is the hallmark of small rectangular junctions with homogeneous current distributions. A maximum  $I_c = 2.2 \mu\text{A}$  at zero applied field was found. The black areas in the peaks of the  $I_c(H_a)$  curves are indicative for the hysteresis in the  $IV$ -characteristics. At the measuring temperature, this junction has a typical  $J_c$  of 29  $\text{A}/\text{cm}^2$ , from which a value for the Josephson

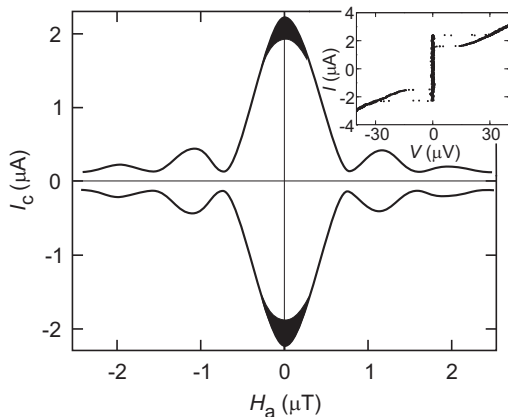


FIG. 2: Critical current  $I_c$  as a function of applied magnetic field  $H_a$  for a  $50 \mu\text{m}$  wide straight  $\text{Nd}_{1.85}\text{Ce}_{0.15}\text{CuO}_4/\text{Nb}$  ramp-type junction ( $T = 4.2 \text{ K}$ ). The dark areas correspond to the hysteresis in the current-voltage characteristic shown for  $H_a = 0$  in the inset.

penetration depth  $\lambda_J = 65 \mu\text{m}$  is estimated. This  $J_c$  is several times larger than attainable with grain boundary junctions. The normal-state resistance for this junction is  $13 \Omega$ , which gives an  $I_c R_n$  product of about  $30 \mu\text{V}$  and  $R_n A = 1.0 \times 10^{-6} \Omega\text{cm}^2$ .

The  $I_c(H_a)$ -dependence for a  $\text{Nd}_{1.85}\text{Ce}_{0.15}\text{CuO}_4/\text{Nb}$  zigzag junction having 8 facets of  $25 \mu\text{m}$  width is presented in Fig. 3(a). Instead of an  $I_c$ -maximum at  $H_a = 0$ , one can observe a maximum  $I_c$  of  $1.8 \mu\text{A}$  at  $H_a = 0.5 \mu\text{T}$ . This zigzag junction shows a highly symmetric  $I_c(H_a)$  pattern for both polarities of current bias and applied magnetic field. The critical current at  $H_a = 0$  falls to less than 32% of its peak value. Presuming that  $J_c$  for this junction is equal to the reference junction described above, the zero field  $I_c$  is only 7% of the expected value for an equally long straight junction, disregarding wide-junction effects. It should be noted that also the maximum  $I_c$  at  $H_a = 0.5 \mu\text{T}$  is 2–3 times lower than expected based on the  $J_c$  of the straight junction. Small variations in the thickness of the Au barrier-layer or the  $\text{Nd}_{1.85}\text{Ce}_{0.15}\text{CuO}_4$  interlayer between the straight junction and the zigzag structure, placed several mm from each other on the chip, may well account for a considerable part of this  $J_c$ -difference. Further, as was shown by Zenchuk and Goldobin [24], a zigzag structure with an odd number of corners is expected to produce spontaneous magnetic flux for all facet-lengths. As the  $I_c(H_a)$ -dependence of Fig. 3(a) is still strongly non-Fraunhoferlike, this spontaneous flux is expected to be smaller than a half-flux quantum per facet length. Nevertheless, a part of the  $I_c$  observed at  $H_a = 0$  and the reduced peak height at  $H_a = 0.5 \mu\text{T}$  may be resulting from this spontaneous flux.

In Fig. 3(b), the  $I_c(H_a)$ -dependence for a zigzag array with 80 facets having a substantially smaller facet length of  $5 \mu\text{m}$  is shown, presenting a maximum  $I_c = 2.0 \mu\text{A}$  at

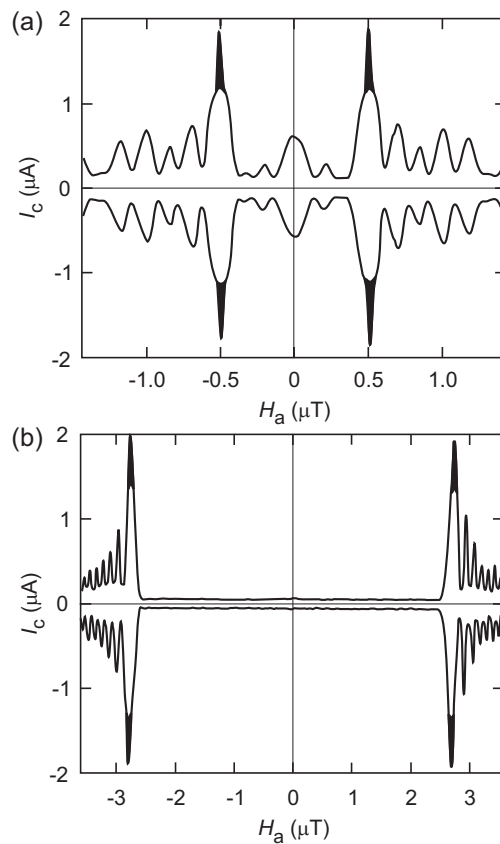


FIG. 3: Critical current  $I_c$  as a function of applied magnetic field  $H_a$  for (a) a  $\text{Nd}_{1.85}\text{Ce}_{0.15}\text{CuO}_4/\text{Nb}$  zigzag array comprised of 8 facets of  $25 \mu\text{m}$  width and (b) a similar array with 80 facets of  $5 \mu\text{m}$  width ( $T = 4.2 \text{ K}$ ).

$H_a = 2.8 \mu\text{T}$ . Also for this very dense zigzag structure the  $I_c(H_a)$ -dependence is highly symmetric. For this structure, a very low ratio of 2% between the critical current at zero magnetic field and the maximal critical current is found.

The  $I_c(H_a)$ -dependencies of these zigzag structures clearly exhibit the characteristic features also seen for the  $\text{YBa}_2\text{Cu}_3\text{O}_7$  case [23], namely the absence of a global maximum at  $H_a = 0$  and the sharp increase in the critical current at a given applied magnetic field. This behavior can only be explained by the facets being alternately biased with or without an additional  $\pi$ -phase change. This provides a direct evidence for a  $\pi$ -phase shift in the pair wave function for orthogonal directions in momentum space and thus for a predominant  $d_{x^2-y^2}$  order parameter symmetry.

If the order parameter were to comprise an imaginary  $s$ -wave admixture, the  $I_c(H_a)$ -dependencies for the zigzag junctions would be expected to display distinct asymmetries, especially for low fields [23]. In addition, the critical current at zero applied field is expected to increase with the fraction of  $s$ -wave admixture. From the high degree of symmetry of the measured characteristics

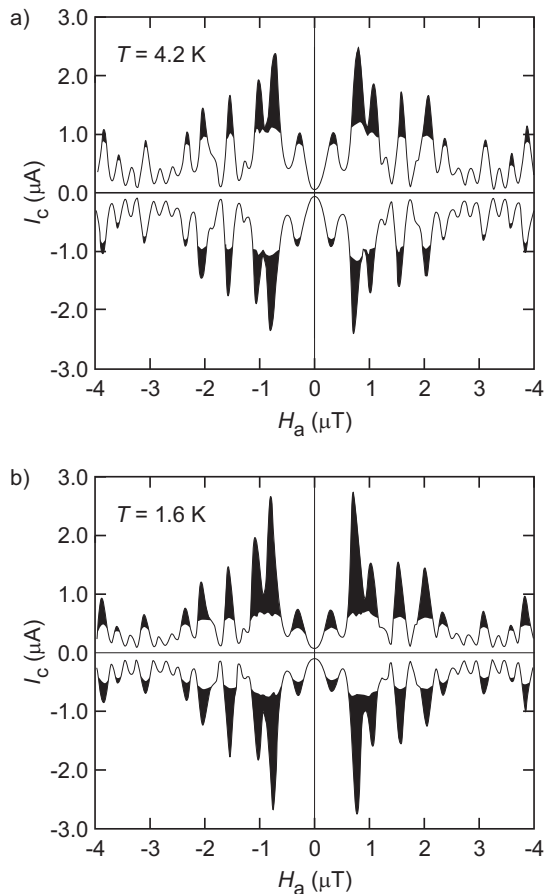


FIG. 4: Critical current  $I_c$  as a function of applied magnetic field  $H_a$  for a  $\text{Nd}_{1.835}\text{Ce}_{0.165}\text{CuO}_4/\text{Nb}$  zigzag array comprised of 8 facets of  $25 \mu\text{m}$  width ( $T = 4.2 \text{ K}$ ) at (a)  $T = 4.2 \text{ K}$  and (b)  $T = 1.6 \text{ K}$ .

of Figs 3(a) and 3(b) and the very low zero field  $I_c$ , no sign of an imaginary  $s$ -wave symmetry admixture to the predominant  $d_{x^2-y^2}$  symmetry can be distinguished.

To investigate a possible change of the order parameter symmetry with doping we have fabricated similar zigzag structures using  $\text{Nd}_{1.835}\text{Ce}_{0.165}\text{CuO}_4/\text{Nb}$  junctions. Figure 4(a) shows the  $I_c(H_a)$ -dependence measured at  $T = 4.2 \text{ K}$  for a structure with 8 facets of  $25 \mu\text{m}$  width. Obviously, also these characteristics indicate a predominant  $d_{x^2-y^2}$ -wave symmetry.

When cooling down the samples to  $T = 1.6 \text{ K}$  all the basic features displayed by the structures at  $T = 4.2 \text{ K}$  remain unaltered, as is shown for the overdoped sample in Fig. 4(b). We thus see no indication for an order parameter symmetry crossover for  $\text{Nd}_{1.85}\text{Ce}_{0.15}\text{CuO}_{4-y}$  in this temperature range, as was recently reported for  $\text{Pr}_{2-x}\text{Ce}_x\text{CuO}_{4-y}$  [22]. Similar results were obtained for optimally doped samples upon cooling down to  $T = 1.6 \text{ K}$ .

In conclusion, our phase-sensitive order parameter symmetry test experiments based on  $\text{Nd}_{2-x}\text{Ce}_x\text{CuO}_{4-y}$

Nb zigzag junctions provide clear evidence for a predominant  $d_{x^2-y^2}$  order parameter symmetry in the  $\text{Nd}_{2-x}\text{Ce}_x\text{CuO}_{4-y}$ . This corroborates the conclusions of studies performed with grain boundary junctions in the optimally doped compounds. To verify various recent reports on possible order parameter changes with overdoping and with decreasing temperature, we have studied the influence of those parameters. No change in the symmetry was observed when overdoping the  $\text{Nd}_{2-x}\text{Ce}_x\text{CuO}_{4-y}$  compound. Further, the order parameter symmetry was found to remain unaltered between  $T = 1.6 \text{ K}$  and  $T = 4.2 \text{ K}$ . This study does not provide an explanation for the contradicting results obtained in other experiments.

The authors thank A. Brinkman, S. Harkema and G. Rijnders for helpful discussions. This work was supported by the Dutch Foundation for Research on Matter (FOM), the Netherlands Organization for Scientific Research (NWO) and the European Science Foundation (ESF) PiShift programme.

\* Permanent address: Department of Physics, Faculty of Mathematics and Sciences, Sepuluh November Institute of Technology, Surabaya 60111, Indonesia

† Present address: CEA-DRT-LETI - CEA/GRE, 17, Av. des Martyrs, 38054 Grenoble Cedex 9, France

‡ Present address: Physikalisches Institut, Universität Tübingen Auf der Morgenstelle 14, D-72076 Tübingen, Germany

- [1] D. J. Van Harlingen, Rev. Mod. Phys. **67**, 515 (1995).
- [2] C. C. Tsuei and J. R. Kirtley, Rev. Mod. Phys. **72**, 969 (2000).
- [3] C. C. Tsuei and J. R. Kirtley, Phys. Rev. Lett. **85**, 182 (2000).
- [4] B. Chesca *et al.*, Phys. Rev. Lett. **90**, 057004 (2003).
- [5] J. W. Ekin *et al.*, Phys. Rev. B **56**, 13746 (1997).
- [6] S. Kashiwaya *et al.*, Phys. Rev. B **57**, 8680 (1998).
- [7] L. Alff *et al.*, Phys. Rev. B **58**, 11197 (1998).
- [8] J. A. Skinta *et al.*, Phys. Rev. Lett. **88**, 207005 (2002).
- [9] M. -S. Kim *et al.*, Phys. Rev. Lett. **91**, 087001 (2003).
- [10] L. Alff *et al.*, Phys. Rev. Lett. **83**, 2644 (1999).
- [11] S. M. Anlage *et al.*, Phys. Rev. B **50**, 523 (1994).
- [12] D. H. Wu *et al.*, Phys. Rev. Lett. **70**, 85 (1993).
- [13] A. Andreone *et al.*, Phys. Rev. B **49**, 6392 (1994).
- [14] N. P. Armitage *et al.*, Phys. Rev. Lett. **86**, 1126 (2001).
- [15] T. Sato *et al.*, Science **291**, 1517 (2001).
- [16] J. D. Kokales *et al.*, Phys. Rev. Lett. **85**, 3696 (2000).
- [17] R. Prozorov *et al.*, Phys. Rev. Lett. **85**, 3700 (2000).
- [18] F. Hayashi *et al.*, J. Phys. Soc. Jpn. **67**, 3234 (1998).
- [19] B. Chesca *et al.*, Condmat-0402131(2003).
- [20] A. Biswas *et al.*, Phys. Rev. Lett. **88**, 207004 (2002).
- [21] M. M. Qazilbash *et al.*, Phys. Rev. B **68**, 024502 (2003).
- [22] H. Balci and R. L. Greene, cond-mat 0402263 (2004).
- [23] H. J. H. Smilde *et al.*, Phys. Rev. Lett. **88**, 057004 (2002).
- [24] A. Zenchuk and E. Goldobin, Phys. Rev. B **69**, 024515 (2004).
- [25] H. Hilgenkamp *et al.*, Nature **422**, 50 (2003).
- [26] H. J. H. Smilde *et al.*, Appl. Phys. Lett. **76**, 912 (2002).